

# D-Wave Checkerboard Order in Cuprates

Kangjun Seo,<sup>1</sup> Han-Dong Chen,<sup>2</sup> and Jiangping Hu<sup>1</sup>

<sup>1</sup>*Department of Physics, Purdue University, West Lafayette, Indiana 47907*

<sup>2</sup>*Department of Physics, University of Illinois at Urbana-Champaign, Urbana, IL 61801*

(Dated: February 6, 2008)

We show that a  $d$ -wave ordering in particle-hole channel, dubbed as  $d$ -wave checkerboard order, possesses important physics that can sufficiently explain the STM results in cuprates. A weak  $d$ -wave checkerboard order can effectively suppress the coherence peak in the single-particle spectrum while leaving the spectrum along nodal direction almost unaffected. Simultaneously, it generates a Fermi arc with little dispersion around nodal points at finite temperature that is consistent with the results of ARPES experiments in the pseudogap phase. We also show that there is a general complementary connection between the  $d$ -wave checkerboard order and the pair density wave order. Suppressing superconductivity locally or globally through phase fluctuation should induce both orders in underdoped cuprates and explain the nodal-antinodal dichotomy observed in ARPES and STM experiments.

PACS numbers: 74.25.Jb, 74.25.Dw, 74.75.-h

Recently, Scanning Tunneling Microscopy (STM) has revealed surprising yet important electronic structures in the high temperature superconductors. The Fourier transform scanning tunneling spectroscopies (FT-STs) from STM have captured two different general features in both momentum and energy spaces<sup>1,2,3,4,5,6,7,8,9</sup>. One feature is dispersive peaks in FT-STs<sup>4,5</sup>, interpreted as interference patterns caused by elastic scattering of quasi-particles from impurities<sup>10</sup>. The other is non-dispersive peaks, a checkerboard modulation observed in various different materials and circumstances. The checkerboard structure was first discovered locally in BSCCO near a vortex core.<sup>1,11</sup> Then, it was found to be a characteristic of the large gap regions where the STM spectrum resembles that in the pseudogap phase.<sup>2,5,7</sup> Later, the STM studies of  $\text{Ca}_{2-x}\text{Na}_x\text{CuO}_2\text{Cl}_2$  revealed the presence of a global long range commensurate checkerboard order independent of doping.<sup>3</sup> Finally, in the pseudogap phase, a similar checkerboard pattern was also observed.<sup>6</sup>

The origin of the checkerboard has become central to understanding the nature of electronic states in cuprates. Various different mechanisms have been considered to explain the observed non-dispersive checkerboard modulation, including pair density modulation<sup>12,13,14,15,16</sup>, current density modulation<sup>17,18</sup>, spin modulation<sup>19</sup>, stripe charge modulation<sup>20,21</sup>, and impurity scattering<sup>22</sup> and so on. Among the proposed mechanisms, the pair density wave (PDW) has been shown to capture important characteristics of the checkerboard density modulation. The mechanism of PDW derives from high pairing energy scale in cuprates. It suggests that unlike the superconductivity of normal BCS type superconductors that can be destroyed by breaking Cooper pairs, the superconductivity in cuprates can be more easily weakened or destroyed by phase fluctuations than by pair breaking. Based on this argument, pair density localization<sup>12</sup> was first proposed to explain the local checkerboard modulation in the presence of impurity or vortex. Later, a global pair density wave (PDW) was proposed to explain

the checkerboard physics in the pseudogap state<sup>6,13</sup>. It has also been shown that the symmetry of the tunneling intensity can distinguish the pair density modulation from the conventional density modulation<sup>13</sup>. While the pair density modulation provides a good understanding of the experimental results, it does not establish a direct link between superconducting and pseudogap states, as is suggested by the presence of the non-dispersive checkerboard density modulation in both states. Furthermore, the theory has not explained three important features present in the STM spectrum: **1.** the density of state at low energy in superconducting state does not change whether or not a checkerboard modulation takes place locally; **2.** the overall intensity of the modulation is rather small; **3.** the small modulation has a large effect on the STM spectrum around the superconducting gap.

In this Letter, we show that an explanation based on  $d$ -wave checkerboard density (DWCB) order in particle-hole channel can overcome the above limitations of the PDW theory. The DWCB can be viewed as a natural extension of the  $d$ -density wave (DDW) order proposed to explain pseudogap physics<sup>23,24</sup>, and is only different from the latter in terms of order wavevectors. We show that the DWCB order must exist when the PDW order is present in the global  $d$ -wave superconducting state. Moreover, we demonstrate that the DWCB, with  $\mathbf{Q} = \{(\pi/2, 0), (0, \pi/2)\}$  and  $f(\mathbf{k}) = \cos(k_x) - \cos(k_y)$ , can explain the STM experimental results. We show that the DWCB order has little effect on the density of state at low energy in the superconducting phase, but has a strong effect on the STM spectrum around the superconducting gap at high energy. This result naturally explains the puzzling dichotomy between the nodal and antinodal regions observed in STM<sup>7</sup> and angle resolved photoemission spectroscopy (APRES)<sup>25</sup>. The DWCB order also preserves in FS-STM spectrum at the wavevector  $\mathbf{Q}$  the same symmetry as that observed in the experiments. Moreover, the DWCB preserves the nodes in the single particle spectrum, and generates a Fermi arc with

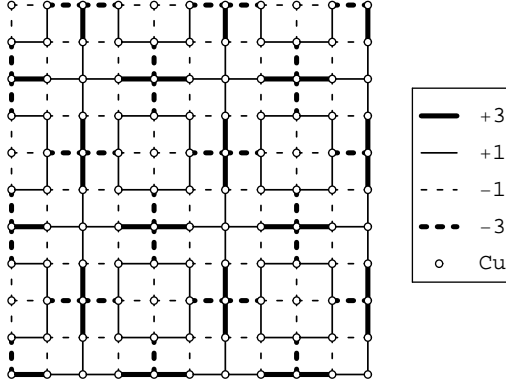


FIG. 1: The configuration of bond density of DWCB order, or  $W_\delta(r)$ . It is manifestly shown that the pattern has  $4a \times 4a$  periodicity and  $d_{x^2-y^2}$  symmetry.

little dispersion around the nodal points at high temperature, which are consistent with the results from ARPES. The Fermi arc has been a signature of the pseudogap region, and has been proposed to explain the checkerboard pattern observed in the pseudogap state<sup>26</sup>. Thus, the DWCB provides a physical origin of the Fermi arc. To our knowledge, this letter presents the first concrete model describing this physics.

*The connection between particle-particle (P-P) and particle-hole (P-H) channel orders:* To illustrate the complementary connection, we make use of the DDW order, since the only difference between the DWCB and DDW orders is the order wavevectors. Let's consider a state with a DDW order,  $\langle \sum_\sigma c_{\mathbf{k}\sigma}^\dagger c_{\mathbf{k}+\mathbf{Q}'\sigma} \rangle = i\Delta_{\text{ddw}} f(\mathbf{k})$ , and a  $d$ -wave superconducting order (DSC),  $\langle c_{\mathbf{k}\uparrow} c_{-\mathbf{k}\downarrow} \rangle = \Delta_{\text{dsc}} f(\mathbf{k})$ , where  $\mathbf{Q}' = (\pi, \pi)$ . Some simple calculation will show that in the above mixed state of DDW and DSC, there naturally exists a PDW order with a wavevector at  $\mathbf{Q}'$ , given by

$$\langle c_{\mathbf{k}\uparrow} c_{-\mathbf{k}+\mathbf{Q}'\downarrow} \rangle \propto i\Delta_{\text{ddw}} \Delta_{\text{dsc}} f^2(\mathbf{k}). \quad (1)$$

This indicates that the mixed state of DDW and DSC has a complementary description as a mixed state of PDW and DSC. It is important to note that the symmetry of the PDW order in this case is an extended  $s$ -wave. It is also easy to see that the symmetries of the order in the P-P channel and that in the P-H channel must be correlated with each other: if one is the extended  $s$ -wave, the other is the  $d$ -wave and vice versa. The above result holds for the DWCB order by replacing  $\mathbf{Q}'$  by  $\mathbf{Q}$ . In a global DSC state, the DWCB order must exist when a checkerboard PDW order is present. The complementary connection suggests that if the phase fluctuation leads to a Cooper pair modulation pattern, orders in both the P-P and the P-H channel have to be simultaneously considered in microscopic models.

*BdG equation and co-existence of PDW and DWCB:* To verify the existence of the DWCB order and the above complementary connection, we perform a self-consistent

BdG calculation. We start from the following general Hamiltonian on a two dimensional square lattice with the nearest-neighbor attractive density interaction,

$$H = -\frac{1}{2} \sum_{\langle ij \rangle} [t_{ij} c_i^\dagger c_j + h.c.] + \sum_{\langle ij \rangle} V_{ij} n_i n_j - \mu \sum_i n_i. \quad (2)$$

The density interaction  $V_{ij}$  includes two parts,

$$V_{ij} = V^0 + \delta V_{\mathbf{r}_i, \mathbf{r}_j} \quad (3)$$

where  $V^0$  favors a  $d$ -wave superconducting state and  $\delta V_{\mathbf{r}_i, \mathbf{r}_j}$  describes a modulating density interaction which creates a small checkerboard modulation on the top of the uniform superconducting state,

$$\delta V_{\mathbf{r}, \mathbf{r}'} = V'_{\mathbf{r}'-\mathbf{r}} (\cos \mathbf{Q} \cdot \mathbf{r} + \cos \mathbf{Q} \cdot \mathbf{r}'), \quad (4)$$

where  $V'_x = V'$  and  $V'_y = -V'$ . The difference on the signs of  $V'_x$  and  $V'_y$  provides us the  $d$ -wave symmetry in the P-H channel order. We also note that the sign difference does not break rotational symmetry with respect to a proper rotation center in the lattice.

Starting with Eq. (2), we can derive the BdG equations by introducing mean-field decoupling of the nearest-neighbor interaction terms and obtain a self consistent solution. The Bogoliubov-de Gennes equation is given by

$$\begin{pmatrix} \hat{H}_0 & \hat{\Delta}^* \\ \hat{\Delta} & -\hat{H}_0^* \end{pmatrix} \begin{pmatrix} u_n(\mathbf{r}) \\ v_n(\mathbf{r}) \end{pmatrix} = E_n \begin{pmatrix} u_n(\mathbf{r}) \\ v_n(\mathbf{r}) \end{pmatrix} \quad (5)$$

where  $\hat{H}_0$  and  $\hat{\Delta}$  are transfer matrices such that

$$\hat{H}_0 \psi_n(\mathbf{r}) = - \left[ \sum_\delta (t + W_\delta(\mathbf{r})) + \mu(\mathbf{r}) \right] \psi_n(\mathbf{r} + \delta) \quad (6)$$

$$\hat{\Delta} \psi_n(\mathbf{r}) = \sum_\delta \Delta_\delta(\mathbf{r}) \psi_n(\mathbf{r} + \delta) \quad (7)$$

where  $\psi_n(\mathbf{r})$  can be either  $u_n(\mathbf{r})$  or  $v_n(\mathbf{r})$ , and  $\delta$  denote nearest-neighbor vectors. The order parameters are self-consistently determined by the self consistent equations: the  $d$ -wave pairing amplitude on a bond  $(\mathbf{r}, \mathbf{r} + \delta)$  is given by

$$\Delta_\delta^{(1)}(\mathbf{r}) = V^0 \langle c_{\mathbf{r}\downarrow} c_{\mathbf{r}+\delta\uparrow} + c_{\mathbf{r}+\delta\downarrow} c_{\mathbf{r}\uparrow} \rangle / 2, \quad (8)$$

the pair density wave order in the P-P channel is

$$\Delta_\delta^{(2)}(\mathbf{r}) = \delta V_{\mathbf{r}, \mathbf{r}+\delta} \langle c_{\mathbf{r}\downarrow} c_{\mathbf{r}+\delta\uparrow} + c_{\mathbf{r}+\delta\downarrow} c_{\mathbf{r}\uparrow} \rangle / 2, \quad (9)$$

and the density order in the P-H channel is

$$W_\delta(\mathbf{r}) = -\delta V_{\mathbf{r}, \mathbf{r}+\delta} \langle c_{\mathbf{r}\sigma}^\dagger c_{\mathbf{r}+\delta\sigma} \rangle. \quad (10)$$

We have numerically solved the BdG equation with various different parameter settings including different band structures in the square lattice with different  $N \times N$  sizes. We find that the co-existence of the PDW and DWCD and the symmetry correspondence between them are the robust results in our calculation for this system.

For example, with a parameter setting,  $V^0 = 2.5t$  and  $V' = t$ , the results are given by, for  $\mathbf{r}' - \mathbf{r} = \hat{x}$  or  $\hat{y}$ ,  $\Delta_{\mathbf{r}'-\mathbf{r}}^{(1)}(\mathbf{r}) = \pm\Delta_0$ ,  $\Delta_{\mathbf{r}'-\mathbf{r}}^{(2)}(\mathbf{r}) = \Delta_1(\cos \mathbf{Q} \cdot \mathbf{r} + \cos \mathbf{Q} \cdot \mathbf{r}')$ , and  $W_{\mathbf{r}'-\mathbf{r}}(\mathbf{r}) = \pm W_0(\cos \mathbf{Q} \cdot \mathbf{r} + \cos \mathbf{Q} \cdot \mathbf{r}')$  with  $\Delta_0 = 0.3t$ ,  $\Delta_1 = 0.25t$ , and  $W_0 = 0.15t$ , which are corresponding to a state with

$$\Delta_{\text{dsc}}(\mathbf{r}) = \Delta_0 \quad (11)$$

$$\Delta_{\text{pdw}}(\mathbf{r}) = \Delta_1 \cos \mathbf{Q} \cdot \mathbf{r} \quad (12)$$

$$W_{\text{dwc}}(\mathbf{r}) = W_0 \cos \mathbf{Q} \cdot \mathbf{r} \quad (13)$$

We note that PDW and DWCB has the same spatial modulation as  $\cos \mathbf{Q} \cdot \mathbf{r}$ , while the symmetries of the PDW and DWCB orders are the extended  $s$ -wave and  $d$ -wave respectively. As shown in Fig. 1, DWCB has  $4a \times 4a$  periodicity and  $d$ -wave symmetry. Similar order parameters have been mentioned in Ref.<sup>22</sup>. The solutions are independent of the initial guesses for the local variables and converge quickly as  $N$  increases.

After demonstrating the co-existence of the DWCB and PDW, now we are interested in the physical effects of the DWCB order. To obtain a clear picture of the DWCB, we illustrated a static pattern of the bond strength of the DWCB order in Fig. 1:

$$W_{\hat{x}}(\mathbf{r}) = \text{Re}(W_0) \left[ \cos \frac{\pi x}{2} - \sin \frac{\pi x}{2} + \cos \frac{\pi y}{2} \right] \quad (14)$$

$$W_{\hat{y}}(\mathbf{r}) = -\text{Re}(W_0) \left[ \cos \frac{\pi y}{2} - \sin \frac{\pi y}{2} + \cos \frac{\pi x}{2} \right] \quad (15)$$

It is clear that the DWCB order has  $4a \times 4a$  periodicity and  $d_{x^2-y^2}$  symmetry. Similar order parameters have been mentioned in Ref.<sup>22</sup>.

Now we numerically calculate the average density of states(DOS),  $\rho(\omega)$ , and the Fourier components,  $\rho_{\mathbf{Q}}(\omega)$ , at the wavevectors of the DWCB order:  $\mathbf{Q} = \{(\pi/2, 0), (0, \pi/2)\}$ , and directly compare them with experimental results. We calculate the above quantities in two situations with different band dispersions. The results are rather general and are insensitive to the bare band structures. First, we performed calculations in the particle-hole symmetric case. For a simple band dispersion, we choose  $t = -125\text{meV}$  and  $\mu = 0$ .  $\Delta_0 = 40\text{meV}$ , which is relevant for underdoped BSCCO. The imaginary part of the self energy  $\eta = 5\text{meV}$  is used for the entire numerical calculation. Fig. 2(a) shows the average DOS( $\mathbf{Q} = (0, 0)$ ) normalized by the non-interacting Fermi liquids. In the absence of DWCB, there are sharp coherence peaks at the energy of superconducting gap. As DWCB order develops, the coherence peaks are suppressed and pushed away while the spectrum at low energy remains unchanged. Fig. 2(b) shows the Fourier components of the local density of states(LDOS) at the wavevectors,  $\mathbf{Q}$ . As expected,  $\rho_{\mathbf{Q}}(\omega)$  is even with respect to  $\omega$ , namely,  $\rho_{\mathbf{Q}}(\omega) = \rho_{\mathbf{Q}}(-\omega)$ . Second, we repeat our calculations with the band dispersion provided by Norman *et al.*<sup>27</sup> and the result is displayed at the inset in Fig. 2(a). The band energy dispersion is now modified

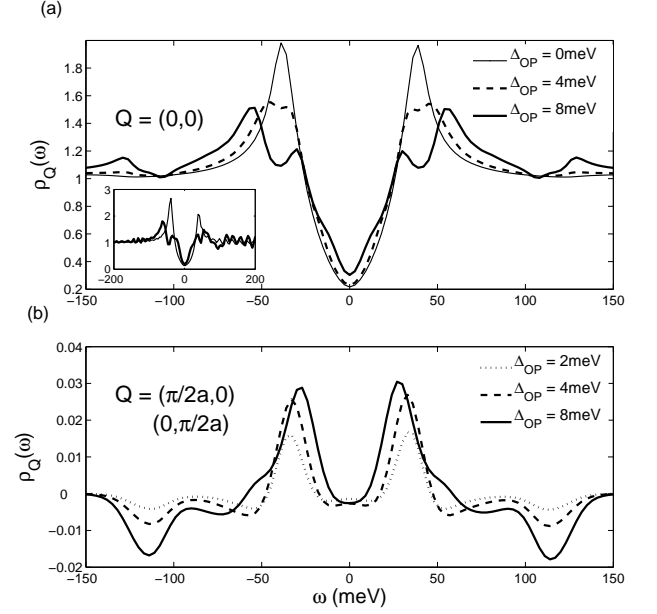


FIG. 2: (a) The average DOS in the particle-hole symmetric case. The inset shows the average DOS with the finite chemical potential included in the band dispersion provided by Norman *et al.*<sup>27</sup>.  $\Delta_{\text{OP}}$  represents  $W_0$ . (b) The Fourier components of LDOS at  $\mathbf{Q} = \{(\pi/2, 0), (0, \pi/2)\}$ .

as such

$$\begin{aligned} \xi_{\mathbf{k}} = & t_1/2(\cos k_x + \cos k_y) + t_2 \cos k_x \cos k_y \\ & + t_3/2(\cos 2k_x + \cos 2k_y) \\ & + t_4/2(\cos 2k_x \cos k_y + \cos k_x \cos 2k_y) \\ & + t_5 \cos 2k_x \cos 2k_y - \mu, \end{aligned} \quad (16)$$

where  $t_1 = -0.5951\text{eV}$ ,  $t_2 = 0.1636\text{eV}$ ,  $t_3 = -0.0519\text{eV}$ ,  $t_4 = -0.1117\text{eV}$ , and  $t_5 = 0.0510\text{eV}$ . The chemical potential  $\mu$  is now set to  $-0.1660\text{eV}$ . Compared with the particle-hole symmetric case, the effect of DWCB on the LDOS is insensitive to the energy band structure. Qualitatively the numerical results are strikingly consistent with experimental results<sup>2,9</sup>, and the large gap region can be represented by the presence of DWCB which is weak at 8-12meV.

Analytically, the general features in STM measurements can be captured by the DWCB. First, due to the anisotropy inherited from the  $d$ -wave factor of pairing, a weak DWCB order has a much stronger effect on the antinodal region than on the nodal region, thus naturally explaining the puzzling dichotomy between the nodal and antinodal excitations in high-temperature superconductors: The local phase fluctuations of Cooper pairs lead to a local modulation of  $d$ -wave ordering in the particle-hole channel, which strongly affects the antinodal single particle excitations. Second, like PDW, DWCB is bond-centered and consequently,  $\rho_{\mathbf{Q}}(\omega)$  is an even function of  $\omega$ , too<sup>13</sup>. The symmetry has been shown to distinguish

the PDW from the typical particle-hole CDW. The existing experimental results are consistent with the even case.

The above result demonstrates the consistency between the DWCB order and the STM experimental results in superconducting state. Now we show that the DWCB order also captures important physics in the pseudogap phase. One important feature of the pseudogap phase is the non-dispersive Fermi arc developed from the nodal point along Fermi surface observed in ARPES<sup>6</sup>. The Fermi arc has been used to explain the STM result in the pseudogap phase<sup>26</sup>. If the pseudogap phase is strongly connected to phase fluctuations of  $d$  wave superconductivity, the single particle spectrum should reflect the DWCB order. Therefore, a robust Fermi arc feature should exist in the mixed DWCB and DSC phases in high temperature. We found that this is indeed the case.

In Fig. 3, we have calculated  $A(\mathbf{k}, \omega)$  in the pseudogap state within the model of Franz and Millis<sup>28</sup>. Fig. 3(a) shows the numerical solutions of the spectral weight,  $A(\mathbf{k}, \omega)$ , as a function of  $\omega$  at high temperature  $T = 120\text{K}$  where  $\Delta_0 = 40\text{meV}$  and the DWCB order is equal to  $8\text{meV}$ . As expected in the pseudogap state, the scattering vector connecting the tips of Fermi arcs unchanged as energy  $\omega$  increases, and is nearly equal to wavevectors of the  $d$ -checkerboard order parameter,  $|\mathbf{Q}| = \pi/2$ . Fig. 3(c) shows the spectral weight at  $\omega = 0$  for the cuts perpendicular to the Fermi arc which matches the experimental results<sup>26</sup>. For the temperature dependence, the length of the Fermi arc is linearly increasing as the temperature rises above  $T_c$ <sup>29</sup>. As seen in Fig. 3(c), at very low temperature the Fermi surface is gapped except for nodal point,  $(\pi/2, \pi/2)$ . As the temperature rises, the gapless region elongates along the Fermi surface, with slight broadening in the direction perpendicular to the Fermi surface.

In summary, the DWCB order offers a unified explanation for the STM experiments in both the superconducting and pseudogap phases. A number of important issues need to be addressed. First, while we show that the complementary connection exists between the  $d$ -wave order in the particle-hole channel and the pair density wave order in the particle-particle channel, the order wavevectors should be determined by microscopic models. In general, the pair fluctuation in different microscopic models can lead to different order wavevectors in the particle-hole channel. For example, the pair fluctuation can be anisotropic in the space that breaks the rotational lattice symmetry, and will result in a stripe-like one dimensional ordering. Second, it is interesting that in a recent renormalization group study of the electron phonon interaction in cuprates, the authors has shown that the DWCB order rises from the coupling to the half breathing or the

$B_{1g}$  phonons<sup>30</sup>. Combining their results with ours suggests that the superconducting phase fluctuations may be strongly coupled with phonons. This hypothesis is of great importance and in need of future investigation. Finally, although a full calculation based on the BDG

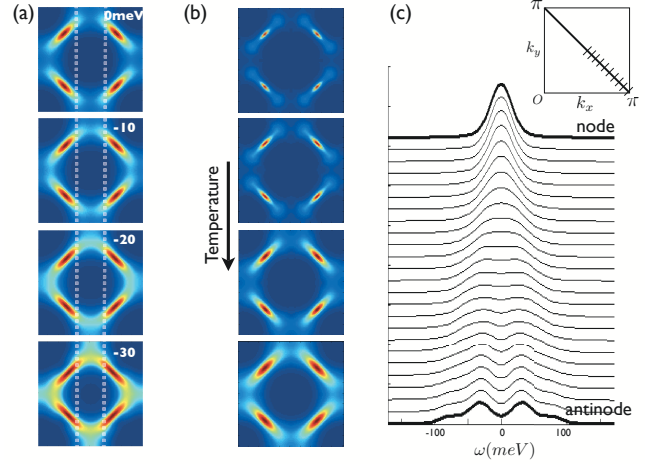


FIG. 3: (a) With DSC and DWCB coexisted, the spectral weights,  $A(\mathbf{k}, \omega)$ , are plotted as a function of  $\omega$  ( $-30\text{meV} \sim 0\text{meV}$ ) in the first Brillouin zone. Here we used  $t = -125\text{meV}$ ,  $t' = \mu = 0\text{meV}$ , and  $T = 120\text{K}$ . Each BZ is segmented by  $100 \times 100$ . White dotted lines indicate the non-dispersive Fermi arcs. (b) Temperature dependence of  $A(\mathbf{k}, \omega)$  at the Fermi level,  $\omega = 0\text{meV}$ . (c) EDC curves from the nodal to antinodal point along the Fermi surface show the gapless region, or Fermi arc.

equation with the DWCB order is yet to be completed, preliminary results show that the qualitative conclusion drawn here should remain valid.

In conclusion, the order in particle hole channel, i.e., the DWCB order, can explain the STM spectrum and the nodal-antinodal dichotomy observed in both STM and ARPES experiments<sup>7,25</sup>. The presence of the DWCB order also preserves the gapless dispersion at nodal points and simultaneously generates a Fermi arc with little dispersion around nodal points at finite temperature. The results are consistent with ARPES experiments and provide an explicit physical explanation of the fermi arc in the pseudogap phase.

J.P.Hu would like to thank Wei-Sheng Lee for helpful discussions. J. P.Hu and K.Seo are supported by Purdue research funding. H.D.Chen is supported by the U.S. Department of Energy, Division of Materials Sciences under Award No. DEFG02-91ER45439, through the Frederick Seitz Materials Research Laboratory at the University of Illinois at Urbana-Champaign.

<sup>1</sup> J. E. Hoffman *et al.*, Science **295**, 466 (2002).

<sup>2</sup> C. Howald, H. Eisaki, N. Kaneko, M. Greven, and A. Ka-

- pitulnik, Phys. Rev. B **67**, 014533 (2003).
- <sup>3</sup> T. Hanaguri *et al.*, Nature (London) **430**, 1001 (2004).
  - <sup>4</sup> K. McElroy *et al.*, Nature (London) **422**, 592 (2003).
  - <sup>5</sup> K. McElroy *et al.*, Physica C **388**, 225 (2003).
  - <sup>6</sup> M. Vershinin *et al.*, Science **303**, 1995 (2004).
  - <sup>7</sup> K. McElroy *et al.*, Phys. Rev. Lett. **94**, 197005 (2005).
  - <sup>8</sup> K. McElroy *et al.*, Science **309**, 1048 (2005).
  - <sup>9</sup> A. C. Fang *et al.*, Phys. Rev. Lett. **96**, 017007 (2006).
  - <sup>10</sup> Q.-H. Wang and D.-H. Lee, Phys. Rev. B **67**, 020511(R) (2003).
  - <sup>11</sup> S. H. Pan *et al.*, Phys. Rev. Lett. **85**, 1536 (2000).
  - <sup>12</sup> H. D. Chen, J. P. Hu, S. Capponi, E. Arrigoni, and S. C. Zhang, Phys. Rev. Lett. **89**, 137004 (2002).
  - <sup>13</sup> H. D. Chen, O. Vafek, A. Yazdani, and S. C. Zhang, Phys. Rev. Lett. **93**, 187002 (2004).
  - <sup>14</sup> H.-D. Chen, S. Capponi, F. Alet, and S.-C. Zhang, Phys. Rev. B **70**, 024516 (2004).
  - <sup>15</sup> Z. Tesanovic, Phys. Rev. Lett. **93**, 217004 (2004).
  - <sup>16</sup> A. Melikyan and Z. Tesanovic, Phys. Rev. B **71**, 214511 (2005).
  - <sup>17</sup> C. Bena, S. Chakravarty, J. Hu, and C. Nayak, Phys. Rev. B **69**, 134517 (2004).
  - <sup>18</sup> A. Ghosal, A. Kopp, and S. Chakravarty, Phys. Rev. B **72**, 220502(R) (2005).
  - <sup>19</sup> S. Sachdev and E. Demler, Phys. Rev. B **69**, 144504 (2004).
  - <sup>20</sup> S. A. Kivelson *et al.*, Rev. Mod. Phys. **75**, 1201 (2003).
  - <sup>21</sup> J. A. Robertson *et al.*, cond-mat/0602675.
  - <sup>22</sup> D. Podolsky, E. Demler, K. Damle, and B. I. Halperin, Phys. Rev. B **67**, 094514 (2003).
  - <sup>23</sup> C. Nayak, Phys. Rev. B **62**, 004880 (2000).
  - <sup>24</sup> S. Chakravarty, R. B. Laughlin, D. K. Morr, and C. Nayak, Phys. Rev. B **63**, 094503 (2001).
  - <sup>25</sup> X. J. Zhou *et al.*, Phys. Rev. Lett. **92**, 187001 (2004).
  - <sup>26</sup> U. Chatterjee *et al.*, Phys. Rev. Lett. **96**, 107006 (2006).
  - <sup>27</sup> M. R. Norman, M. Randeria, H. Ding, and J. C. Cam-puzano, Phys. Rev. B **52**, 615 (1995).
  - <sup>28</sup> M. Franz and A. J. Millis, Phys. Rev. B **58**, 14572 (1998).
  - <sup>29</sup> A. Kanigel *et al.*, Nature Physics **2**, 447 (2006).
  - <sup>30</sup> H. C. Fu, C. Honerkamp, and D.-H. Lee, cond-mat/0509072.